

Available online at www.sciencedirect.com

jmr&t
Journal of Materials Research and Technology
journal homepage: www.elsevier.com/locate/jmrt



Original Article

Tensile, three-point bending and impact strength of 3D printed parts using PLA and recycled PLA filaments: A statistical investigation



Gurcan Atakok ^{a,*}, Menderes Kam ^b, Hanife Bukre Koc ^c

^a Department of Mechanical Engineering, Faculty of Technology, Marmara University, Maltepe, 34854 Istanbul, Turkey

^b Department of Mechanical and Metal Technologies, Cumayeri Vocational School, Düzce University, 81700 Düzce, Turkey

^c Institute of Pure and Applied Sciences, Marmara University, Kadıköy, 34722 Istanbul, Turkey

ARTICLE INFO

Article history:

Received 29 December 2021

Accepted 3 March 2022

Available online 10 March 2022

Keywords:

FDM

Re-PLA

Taguchi

Three-point bending strength

SEM

ABSTRACT

In this study, the Taguchi methodology was used to investigate the effects of Fused Deposition Modeling (FDM) production parameters tensile strength, three-point bending strength, and impact strength of three-dimensional (3D) printed polylactic acid (PLA) and recycled polylactic acid (Re-PLA) test parts. As FDM process parameters, filaments (PLA, Re-PLA), three different layer thicknesses (0.15–0.20–0.25 mm), occupancy rates (30%, 50% and 70%), and filling structure (Rectilinear) were determined in the experimental design. The FDM technique was used to print the test parts. The tensile, three-point bending, and impact strength of the test parts were determined using the ISO 527, ISO 180, and ISO 178 test standards, respectively. The results showed that layer thickness is the most efficient factor for improving tensile strength, three point bending strength, and impact strength rather than occupancy rate or filament materials. The optimum results were obtained in layer thickness (0.25 mm), occupancy rate (70%), and filament material (PLA), respectively. They were calculated to be as 60.006 MPa at tensile strength, 125.423 MPa at three-point bending strength, 16.961 kJ/m² at izod impact strength. Also, Scanning Electron Microscopy (SEM) has been utilized to investigate the morphology and topography alterations in the fractured surface of test parts. The study demonstrates the possibility of 3DP with Re-PLA filament and environmental awareness was noted by using recycled filament. The study demonstrates the possibility of 3DP with Re-PLA filament and environmental awareness was noted by using recycled filament. The research shows that 3D printing with Re-PLA is feasible.

© 2022 The Authors. Published by Elsevier B.V. This is an open access article under the CC BY license (<http://creativecommons.org/licenses/by/4.0/>).

* Corresponding author.

E-mail addresses: gatakok@marmara.edu.tr (G. Atakok), mendereskam@duzce.edu.tr (M. Kam), hbukre@gmail.com (H.B. Koc).

<https://doi.org/10.1016/j.jmrt.2022.03.013>

2238-7854/© 2022 The Authors. Published by Elsevier B.V. This is an open access article under the CC BY license (<http://creativecommons.org/licenses/by/4.0/>).

1. Introduction

3D printing (3DP) is one of the rapid prototyping (RP) techniques of products based on computer-aided 3D modeling [1]. It also enables an initial and effective design process for successful and efficient end products [2]. As a result, it comes to the forefront as a driving force in material savings in the production process [3]. It has been suggested that 3DP technology can revolutionize manufacturing practices in many industries [4,5]. 3DP has gained popularity in recent years as a result of its ability to reduce the amount of time and material used in the manufacturing process [6]. RP, functional part production, and free form production are all production types that benefit from 3DP technology [7]. FDM is the most commercialized 3DP or another name Rapid Prototyping technology currently [8]. The FDM process, as seen in Fig. 1, works on the premise of adding layer by layer plastic filament material [9,10].

The following are highly preferred Additive Manufacturing (A.M.) technologies that generate similar logic using different methods: Selective Laser Sintering (SLS) [13], Selective Laser Melting (SLM), Stereolithography (SL) or Selective Laser Apparatus (SLA), Laminated Object Manufacturing (LOM) [14], and Electron Beam Melting (EBM). Furthermore, research has discovered two alternative methodologies known as Fused Particle/Granule Fabrication (FPF/FGF) [15] and Interpretive Structural Modeling (ISM) [16]. At the end of this production, waste parts and residues are formed. Re-introducing waste raw material into the production chain is one of the best approaches to increase efficiency and control waste during production [17].

In the twenty-first century, “cheap raw material” is the equivalent of “waste” [18]. Therefore, studies involving recycling in the literature support this. As a result, the utilization of recycled filament was highlighted.

Known to be biodegradable, biocompatible and cost-effective, PLA is a thermoplastic that is commonly used for FDM [19]. However, PLA is the most widespread raw material used in FDM-based 3DP process due to its biodegradability and environmental friendliness [20,21]. PLA, which has a lower molecular weight and lower polymer strength, became the world's second most consumed bioplastic in 2010 due to its

wide applicability [22]. The mechanical qualities of 3D printed parts must be optimized for all of these prospective uses [17,18,23,24].

As a result of their review, Atakok et al. (2021) suggested that according to the literature researches of production techniques and filament materials used, the most preferred parameters are FDM production method and PLA filament, respectively. The reason why PLA filament is widely preferred is its convenience to be recycled compared to other filaments. Therefore, the study supports the use of PLA filament material, after it becomes waste in the next 3D process, because PLA filament is a low-cost raw material [25].

Matsuzaki et al. (2016) found that the material created by adding 6.6 percent carbon to PLA filament had a tensile strength of 185.2 MPa, which enhanced the material's tensile strength [26]. With the inclusion of jute at the same contribution rate, Kam et al. (2020) reached a tensile strength (57.1 MPa) that was equivalent to pure PLA filament (6.1%). In addition, the kind of additive and the ratios of additives are extremely critical in influencing the mechanical properties of the material. Adding different amounts of the similar type of additive to the similar filament can cause considerable changes in the material's mechanical properties. However, increasing quantity of the additive does not always imply that the material will become stronger [27].

Kam et al. (2021) investigated of used for PLA + filament material that has been modified which is used experimental design. In the production of the test parts to be used in the experiments; filling structures (Rectilinear, Triangular, and Full Honeycomb), occupancy rates (10%, 30%, and 50%) and table orientation (0°, 60°, and - 45°) parameters were determined as variables. According to the data obtained in the experiments, the occupancy rate was found to be directly proportional to the tensile strength and Izod impact values [28]. The experimental design was used in another study on PLA material. During the process, layer thickness, material deposition rate, occupancy rate and filling structures are taken into account. According to them, the layer thickness parameter significantly affects the tensile strength [28,29].

Scientists use optimization to decrease the amount of change in a product by managing characteristics and features

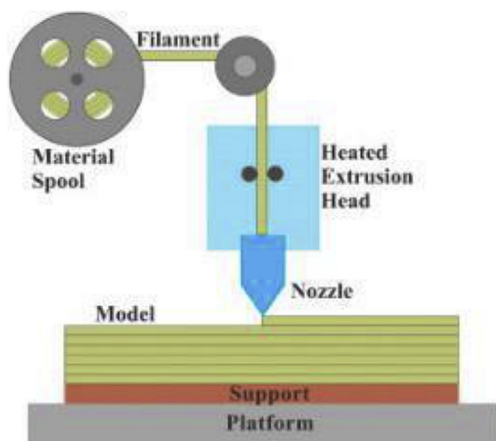


Fig. 1 – Schematic illustration of FDM method [11,12].

Table 1 – FDM system parameters and properties.

No	Properties	Values
1	Printing Method	FDM
2	Printing Size (mm)	220 × 220 x 250
3	Machine Size (mm)	440 × 410 x 465
4	Filament Diameter (mm)	1.75
5	Filament Type	PLA, Re-PLA
6	Diameter of Nozzle (mm)	0.4
7	Temperature of Nozzle (°C)	200
8	Temperature of Bed (°C)	60
9	Printing speed (mm/min)	3000
10	Model	Crealty Ender 3 Pro
11	Slicer Program	Simplify3D
12	CAD Program	Solidworks
13	Tolerance	±0.1
14	Filling Structure	Rectilinear
15	Occupancy Rate (%)	30, 50, 70
16	Layer thickness (mm)	0.15–0.20 - 0.25

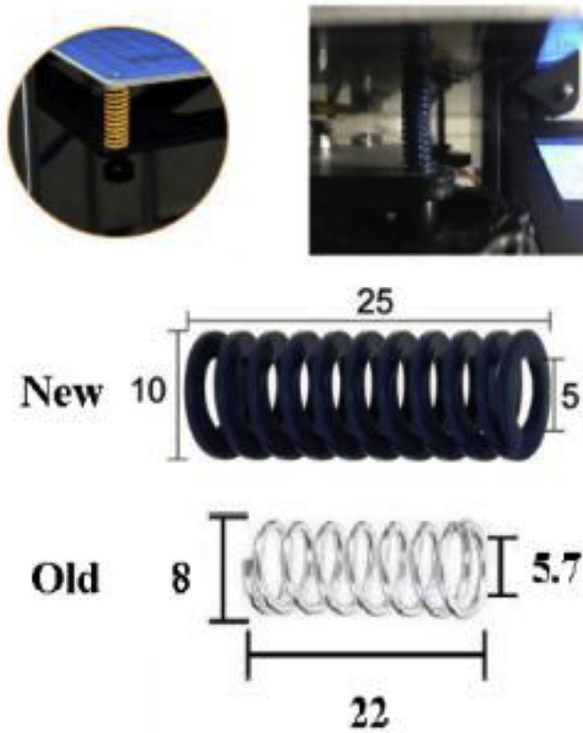


Fig. 2 – Bed springs for stabil bed level.

connected to its design and development. Without a doubt, the input parameters chosen have a significant impact on the final performance of a product. Many methods are commonly used by scientists to create the experimental setup, such as

Orthogonal Array of Taguchi. The experimental data is analyzed to obtain the optimum parameters. Also the significant parameters that have the greatest effect on the final results for study [28,30,31].

The most effective two 3DP characteristics for the strength of items printed using the 3DP process, according to the literature, are the filling structure and occupancy rate [30–37].

The average tensile strength increases proportionally as the occupancy rate increases with each filling structures. Izod impact levels vary independently of parameters in a rectilinear filling structure. It is not appropriate to work at a 30% occupancy rate or lower in applications where Izod impact values are critical [28].

In this study, the strengths of tensile, izod impact and three-point bending test parts printed with Rectilinear filling structure, layer thicknesses of 0.15–0.20–0.25 mm, 30, 50, 70% occupancy rates were investigated. The S/N ratio was calculated using the Taguchi methodology. The test results were evaluated. Tensile, three-point bending and izod impact tests were performed to determine the mechanical characteristics of the printed test parts relating to strength and hardness. Additionally, the effects of the process parameters were discussed in detail by evaluating the SEM micrographs taken from the fracture surfaces of the tensile test parts as a result of the test. Finally, the results and extensions of this study are summarized.

2. Material and method

Test parts were created in Solidworks Computer Aided Design (CAD) program and then converted to G-code using the Simplify3D slicer program. Tensile test parts in accordance with

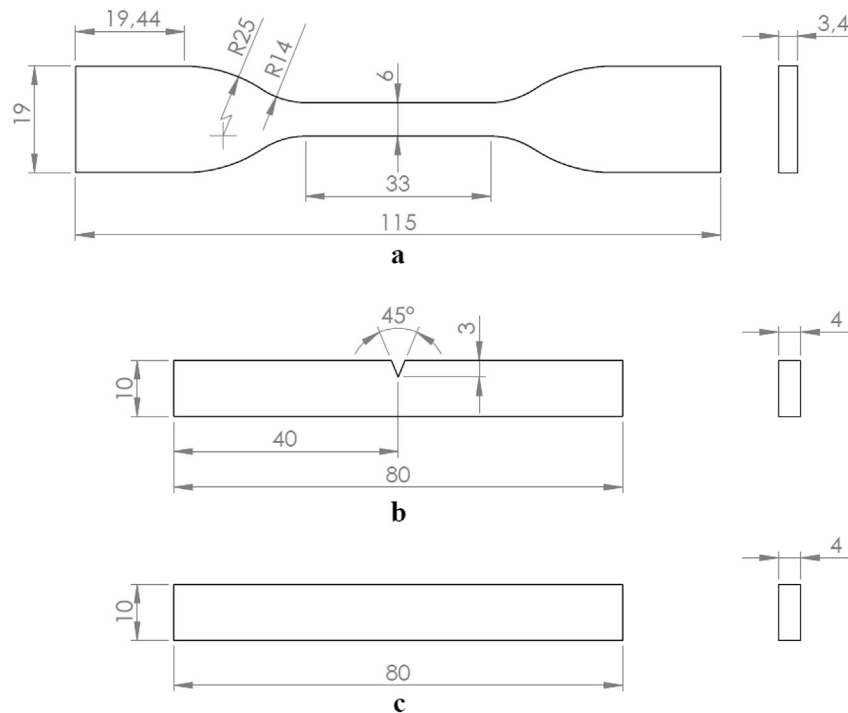


Fig. 3 – (a) ISO 180—Type I tensile strength test standards and (b) ISO 527-Type IV impact strength test standards (c) ISO 178 three point bending test standards (all measurements are in mm).

Table 2 – Properties of filament materials and test results [42].

Properties	Values
Material	PLA, Re-PLA
Filament Colour	Black
Diameter of Filament (mm)	1.75
Temperature of Bed (°C)	60–75
Extruding Temperature of PLA (°C)	200–220
Extruding Temperature of Re-PLA (°C)	190–215
Tensile Strength of PLA (MPa)	56
Tensile Strength of Re-PLA (MPa)	63

ISO 527 Type IV [38] standards, Izod impact test parts in accordance with TS EN ISO 180 Type I [39] standards, and three-point bending test parts in accordance with ISO 178 [40] standards were tested with Porima3D PLA and their recycled version Re-PLA filaments. Table 1 lists the FDM system parameters and 3D printer properties.

The Creality Ender 3 Pro was chosen since it is one of the most suitable and high-quality devices for individual usage on the market in terms of price/performance. The accurate alignment of the 3D printer's elements during setup is a crucial requirement for high-quality 3DP [41]. Therefore, component prints were completed following minor upgrades and calibration operations to ensure long-term print quality. First of all, for the device upgrade process; 4 new quality springs were supplied and replaced with normal springs in the device. As a result, the bed level and stability have become more firm. In addition, this change reduced the frequency of prepress calibration processes, minimizing the time lost from manual bed calibration that breaks down after each print. Bed springs for stabil bed level and dimensions are given in Fig. 2.

Figure 3 shows the dimensions of the impact strength test parts (ISO 180—Type I), tensile test part (ISO 527—Type IV), and three point bending test part (ISO 178). Also, Properties of filaments and their values are given in Table 2.

PLA is one of the most widely used FDM thermoplastics, and it's simple to use as a filament in a 3D printer that uses the FDM [43]. PLA filament was chosen since it is the most

commonly encountered filament in the literature when it comes to recycling when compared to other filament types. PLA is also a biodegradable thermoplastic polyester material made from cleaner sources, with less hazardous components and lower 3DP temperatures, which saves energy [28]. Because Porima3D brand filament material is a high-quality brand on the market, it was chosen for PLA and Re-PLA.

Figure 4 shows the images of test parts after all tests for take SEM.

a) Tensile strength test parts b) Impact strength parts c) Three point bending test parts.

In order to avoid confusion between the test parts for SEM analysis, each test part was marked as A (three-point bending test), B (tensile test), and C (Izod impact test), respectively (Fig. 4). Also, the repeated productions of the test parts were carried out according to Table 3.

Tensile tests were carried out on the Zwick Roell Z010 brand tensile test machine seen in Fig. 5.

The determination of the appropriate levels of the factors was made using the Taguchi method. Experiments were designed and performed using L₁₈ one of the Taguchi orthogonal arrays, and the appropriate levels of the factors were determined by analyzing the experimental results [44]. This design L₁₈ has one factor with two levels and many

Table 3 – Repetitive production table for test parts.

Filling structure	Filament	Layer thickness (mm)	Occupancy rate (%)
Rectilinear	PLA/Re-PLA	0.15	30
			50
			70
		0.20	30
			50
			70
		0.25	30
			50
			70

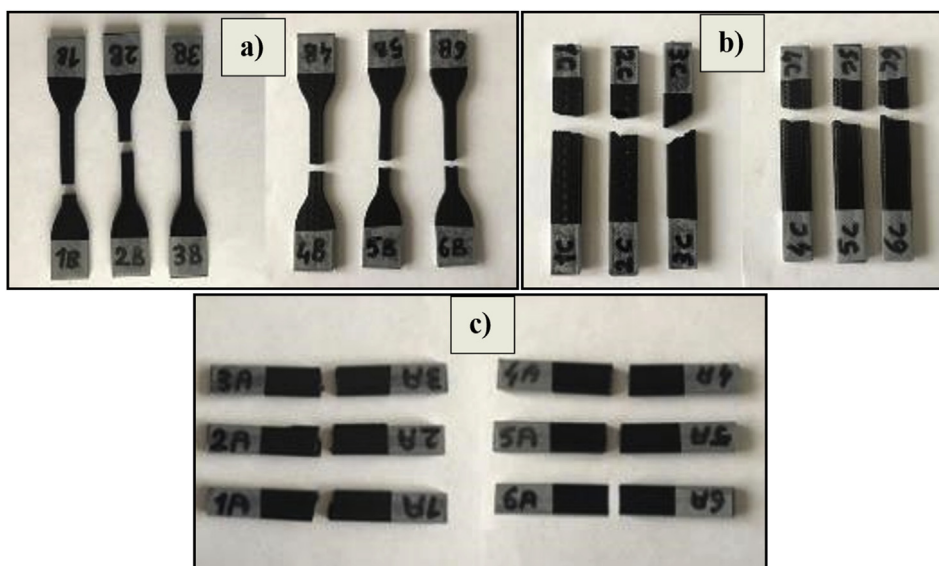


Fig. 4 – Images of test parts after all tests for take SEM.

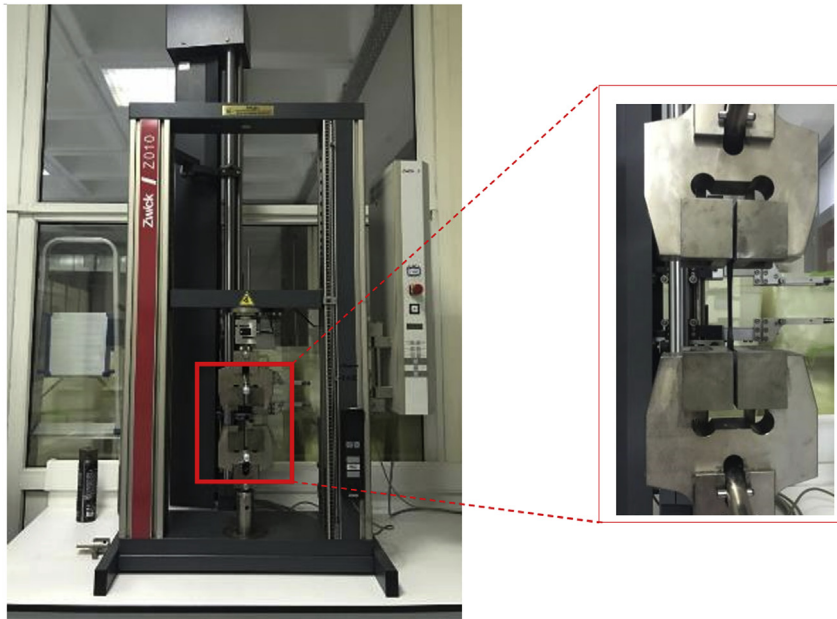


Fig. 5 – Tensile test machine.

Table 4 – Tensile factors and levels of control (Taguchi L_{18}).

No	Factors	Symbol	Unit	Level 1	Level 2	Level 3
1	Filament material (PLA:1; Re-PLA: 2)	A	–	1	2	–
2	Layer thickness (mm) 0.15, 0.20, 0.25	B	mm	1	2	3
3	Occupancy rate (%) (30: 1; 50: 2; 70: 3)	C	%	1	2	3

factors with three levels each. There are 18 rows in all [45]. Control factors and levels for Taguchi L_{18} are given in Table 4.

The values for the occupancy rate are determined as follows: 30, 50 and 70%. This is since when the occupancy rate surpasses 50%, printing times rise majorly despite increased properties of

mechanical, and costs of producing surpassed tolerable bounds. Values below 25% occupancy rate are ineffectual in terms of strength, and the reduction in printing time is minimal. In terms of mechanical qualities, filling structures of honeycomb and rectilinear are the most extensively utilized ones [46].

Table 5 – Taguchi L_{18} orthogonal array Test results and S/N ratios.

No	A	B	C	Tensile strength values (MPa)	S/N (dB)	Impact strength values (kJ/m^2)	S/N (dB)	Bending strength values (MPa)	S/N (dB)
1	PLA	0.15	30	40.23	32.0910	10.90	20.7485	91.00	39.1808
2	PLA	0.15	50	41.16	32.2895	12.36	21.8404	99.40	39.9477
3	PLA	0.15	70	43.86	32.8414	13.70	22.7344	107.66	40.6411
4	PLA	0.20	30	46.46	33.3416	12.96	22.2521	102.00	40.1720
5	PLA	0.20	50	49.40	33.8745	13.73	22.7534	110.66	40.8798
6	PLA	0.20	70	50.10	33.9968	16.13	24.1527	119.66	41.5590
7	PLA	0.25	30	52.93	34.4740	14.02	22.9350	109.00	40.7485
8	PLA	0.25	50	56.90	35.1022	15.00	23.5218	120.66	41.6313
9	PLA	0.25	70	64.93	36.2489	17.04	24.6294	125.00	41.9382
10	Re-PLA	0.15	30	38.10	31.6185	10.50	20.4238	85.43	38.6322
11	Re-PLA	0.15	50	40.03	32.0477	11.26	21.0308	92.50	39.3228
12	Re-PLA	0.15	70	41.03	32.2620	12.13	21.6772	106.00	40.5061
13	Re-PLA	0.20	30	45.66	33.1907	11.38	21.1228	89.96	39.0810
14	Re-PLA	0.20	50	47.20	33.4788	12.46	21.9104	98.74	39.8899
15	Re-PLA	0.20	70	48.43	33.7023	13.55	22.6388	111.33	40.9322
16	Re-PLA	0.25	30	49.20	33.8393	13.86	22.8353	95.60	39.6092
17	Re-PLA	0.25	50	51.50	34.2361	14.96	23.4986	100.83	40.0718
18	Re-PLA	0.25	70	59.40	35.4757	16.40	24.2969	113.00	41.0616

Table 6 – ANOVA for S/N ratios.

Factor	Degree of Freedom (DF)	Sum of Squares (SS)	Mean Square (MS)	F value	P value	Contribution (%)
A	1	35.90	35.899	7.21	0.020	4.07
B	2	682.40	341.199	68.52	0.000	77.29
C	2	104.83	52.417	10.53	0.002	11.87
Residual Error	12	59.76	4.980			6.77
Total	17	882.89				100.00

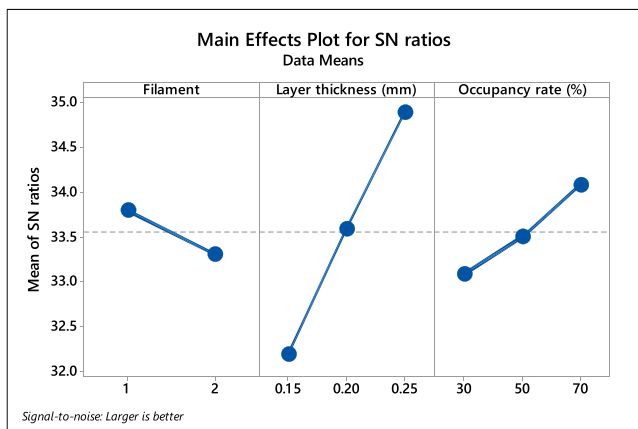


Fig. 6 – S/N rates for tensile strength.

3. Result and Discussion

Using the Taguchi Method, the design of test parameters is the conversion of objective values into the S/N ratio, also known as the quality characteristic evaluation index [47]. Taguchi and Phadke (1989), classify factors as control and noise factors. Factors determined by the designer are control factors. Factors other than these, such as ambient humidity and temperature, are called noise factors. In the Taguchi method, signal to noise (S/N ratio) is used to obtain a robustness system and to desensitize the process to noise factors. Thanks to the use of the S/N ratio, optimum quality design can be achieved with extraordinarily little variation. S/N ratio; It is especially useful in factor weighting, reducing crossover action, the processing means and variation simultaneously, and improving quality. This study aims to optimize the mechanical properties of PLA and Re-PLA parts produced using

variable layer thickness and occupancy rate. For this reason, the larger is better feature is used. As a result, the strength values obtained as a result of the mechanical tests presented in Table 5 are expected to be large and the S/N ratio (η) is used in the 'larger is better' equation. Equation (1) [48].

$$\eta = -10 \log \frac{1}{p} \left[\sum_{i=1}^p \frac{1}{w_i^2} \right] \tag{1}$$

where η is the S/N ratio; w_i is the i th result of the experiment; and p is the repeated times of a trial.

3.1. Tensile strength

The effects of factors and interactions obtained as a result of ANOVA are presented in Table 6 [49]. A regression analysis was used to estimate the results of the studies. Variables B and C were statistically significant. In Fig. 6, the main effect graph for the effects and levels of the parameters is intuitively shown. The effect of the layer thickness value is high compared to other test parameters. In this case, it increases the effectiveness of the layer thickness value on mechanical effects [50]. It is important to have strong mechanical properties in 3DP [46,51]. (2) gives the linear regression equation for estimating tensile strength with a 95% confidence interval (CI). The effect of the layer thickness parameter on the tensile strength is 77.29% and the occupancy rate is 11.87%. It is understood as a result of the tests and statistical analyses that the effect of other variables on the tensile strength is low.

Estimated tensile strength MPa

$$= 14.90 - 2.824 \times A + 150.7 \times B + 0.1465 \times C \tag{2}$$

In equation (2); the numerical values for B and C can be set as mm and %, respectively.

The number should only be used as 1 for PLA filament and 2 for Re-PLA filament material. Filament type, layer thickness,

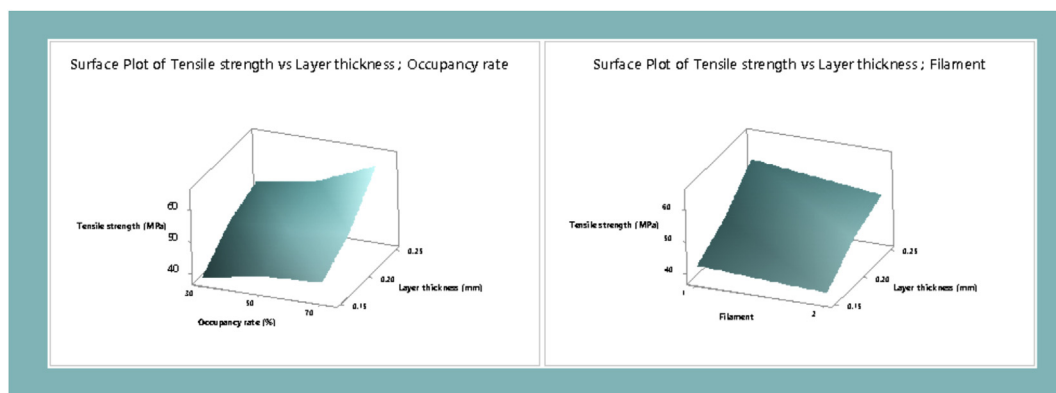


Fig. 7 – Surface plot of tensile strength.

Table 7 – Response table for S/N ratios (Larger is better).

Level	A Filament	B Layer thickness (mm)	C Occupancy rate (%)
1	33.81	32.19	33.09
2	33.32	33.60	33.50
3	–	34.90	34.09
Delta	0.49	2.70	1.00
Rank	3	1	2

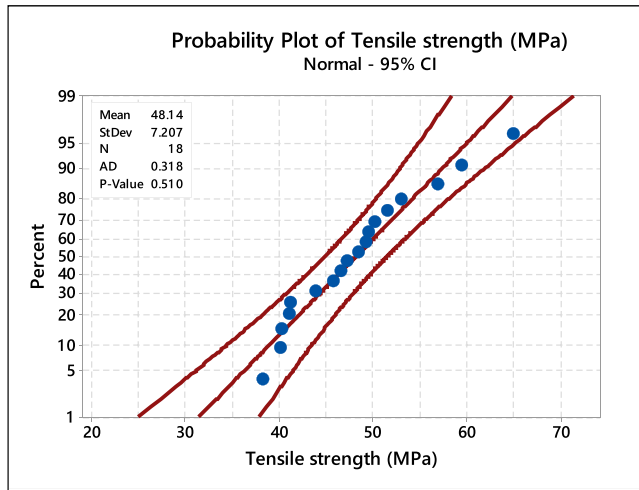


Fig. 8 – Probability plot.

occupancy rate were the most critical factors in determining the tensile strength values. ANOVA corrects the results from the tensile test. PLA and Re-PLA filament were used to obtain optimum tensile strength values of FDM process parameters at third level of layer thickness (B₃), first level of filament (A₁), third level of occupancy rate (C₃). Fig 6 shows the main effect graph for process parameters, S/N ratios and tensile strength. For the optimum tensile strength, printing process parameters (filament material, layer thickness, and occupancy rates) were 0.25 mm, 70%, and PLA, respectively. As a result of using these values, as indicated in Table 5, the best tensile strength value was obtained as 64.93 MPa after using PLA filament. In this case, it shows that it has higher strength than other conditions. The tensile strength data plotted in the surface plot graph is shown in Fig. 7.

The layer thickness, occupancy rates, and filament material were the most critical elements, respectively for the

mechanical qualities (tensile strength values), as shown in Table 7.

The tensile strength values increased proportionally depending on the layer thickness and occupancy rate (Fig. 8). Another parameter, the filament material, has an improvement in tensile strength. The results obtained are consistent with the literature [27,46,51,52]. The surface plot graph shows the layer thickness and occupancy rate parameters that have the greatest influence on the tensile strength value. The effects of production parameters on tensile strength are presented by comparing them. The normal probability graph of the tensile strength obtained as a result of the modeling is presented in Fig. 8. The accuracy of the model can be checked using this graph. Since the P-values of the normality graph are above 0.05 and the residuals follow a normal distribution, it is understood that the experimental study and the mathematical model are compatible. In addition, the fact that the distribution is close to the central axis shows that the experimental model is balanced and correct.

3.2. Impact strength

Considering the P value given in the ANOVA results in Table 8, the layer thickness and occupancy rate were statistically significant. Equation (3), obtained as a result of linear regression, is given in order to estimate the impact strength values.

$$\text{Estimated Impact strength value (kJ/m}^2\text{)} = 5.016 - 1.038A + 34.05 \times B + 0.06387 \times C \tag{3}$$

Figure 9, the main effects plot, shows the levels of the factors used. The impact strength value can be estimated using the Linear Regression Equation (3). The layer thickness parameter has an effect of 55.75% on the impact resistance values, and the occupancy rate has an effect of 31.73%. It is seen that the effectiveness of the layer thickness value on the impact resistance is almost two times higher than the occupancy rate. Strength of 17.04 MPa was obtained from PLA filament using 0.25 mm layer thickness and 70% occupancy rate, and it is the highest strength value among the tests performed. As a result of the use of Re-PLA filament, a layer thickness of 0.25 mm and strength of 16.40 MPa were obtained at 70% occupancy rate. The maximum impact strength value obtained from PLA filament is 0.4% higher than the maximum impact strength obtained using Re-PLA filament. Other factors have little effect on impact strength values.

Table 9 shows the response table for S/N ratios (Larger is better).

Table 8 – ANOVA for S/N ratios (Impact strength).

Factor	Degree of Freedom (DF)	Sum of Squares (SS)	Mean Square (MS)	F value	P value	Contribution (%)
A	1	4.846	4.8464	19.49	0.001	7.75
B	2	34.863	17.4317	70.10	0.000	55.75
C	2	19.839	9.9195	39.89	0.000	31.73
Residual Error	12	2.948	0.2487			4.77
Total	17	62.533				100.00

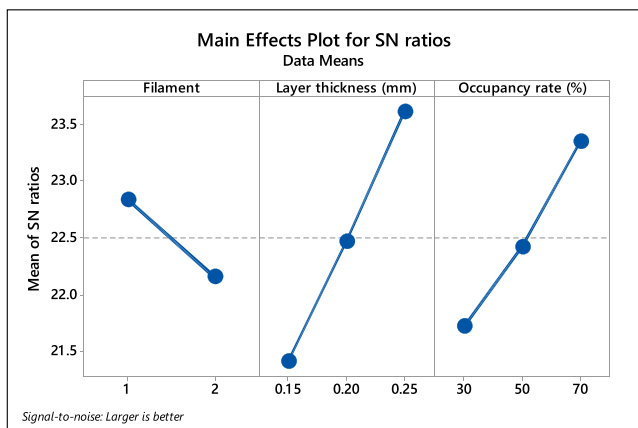


Fig. 9 – S/N rates for impact strength.

Table 9 – Response table for S/N ratios (Larger is better).

Level	A Filament	B Layer thickness (mm)	C Occupancy rate (%)
1	22.84	21.41	21.72
2	22.16	22.47	22.43
3	–	23.62	23.35
Delta	0.68	2.21	1.64
Rank	3	1	2

The B and C values can be selected in mm and % as (3) in the equation. Number A should only be used as 1 for PLA and 2 for Re-PLA filament.

By using PLA and Re-PLA filaments, the use of FDM process parameters such that the layer thickness is at the third level (B₃), the type of filament material is at the first level (A₁) and the occupancy rate is at the third level (C₃) has provided optimum izod impact strength. The effect of FDM parameters on impact strength is shown in the graph of S/N ratios given in Fig. 9. The parts produced using the PLA (1) filament with a layer thickness of 0.25 mm and an occupancy rate of 70% exhibited the best impact resistance values. Surface plot graphics of impact strength values are shown in Fig. 10.

The surface plot graph shows the effectiveness of the parameters that influence the impact strength. The parameters

that have a greater effect on impact resistance are layer thickness and occupancy rate, respectively. The efficiencies of the parameters on the surface images were compared. And it is understood that there is a direct proportional relationship between the parameters and the impact resistance value.

The interaction values obtained by modeling as a result of the test are presented in Table 8. The normal probability graph of the impact strength obtained as a result of the modeling is presented in Fig. 11. Since the p values of the normality graph are above 0.05 and the residuals follow a normal distribution, it is understood that the experimental study and the mathematical model are compatible. In addition, the distance of the distribution from the center axis is an indicator of the stability and accuracy of the established model. Since there is a balanced distribution, the established model is correct.

As the probability plot layer thickness and occupancy rates increase, the impact resistance value also increases (Fig. 11).

3.3. Bending strength

Considering the P value given in the ANOVA results is presented in Table 10. The layer thickness, occupancy rate, and filament materials were statistically significant. The linear regression equation is given in (4) for the estimated three-point bending strength value.

$$\text{Estimated three – point bending strength (MPa)} = 69.42 - 10.18 \times A + 136.8 \times B + 0.4569 \times C \quad (4)$$

Figure 12 shows the main effect plot for the effects and levels of the three point bending strength parameters used in the model. Mechanical characteristics of high quality are required. The three-point bending strength value can be estimated using the Linear Regression Equation (4). The layer thickness parameter has a 26.46% and filament material has a 21.61% effect on the three-point bending strength values, whereas the occupancy rate has a 46.53% effect. Other factors have a minor impact on impact strength values. B and C values can be selected numerically as mm and % in Equation (4). Number A should be used for filament only and should be 1 for PLA and 2 for Re-PLA. The ANOVA verified the results of the three-point bending strength values. Layer thickness, occupancy rates and filament material are 0.25 mm–70% and PLA optimum process parameters, respectively. These parameters

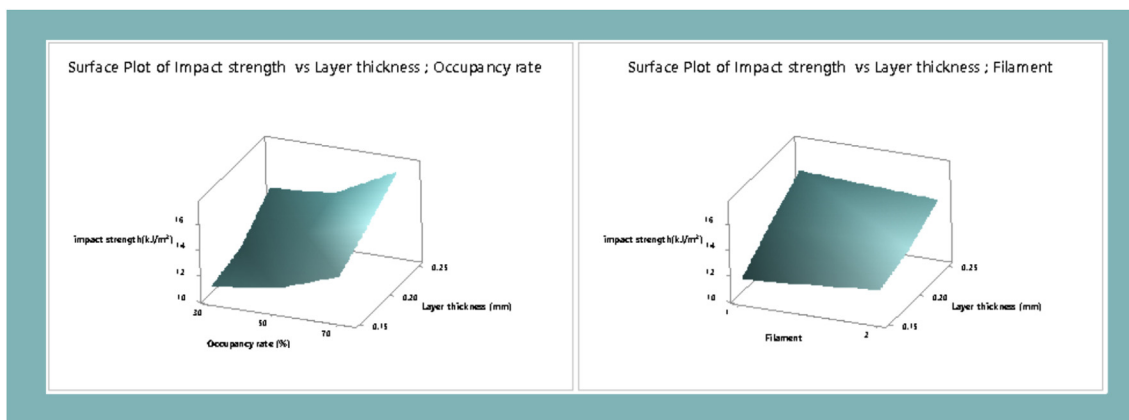


Fig. 10 – Surface plots of impact strength.

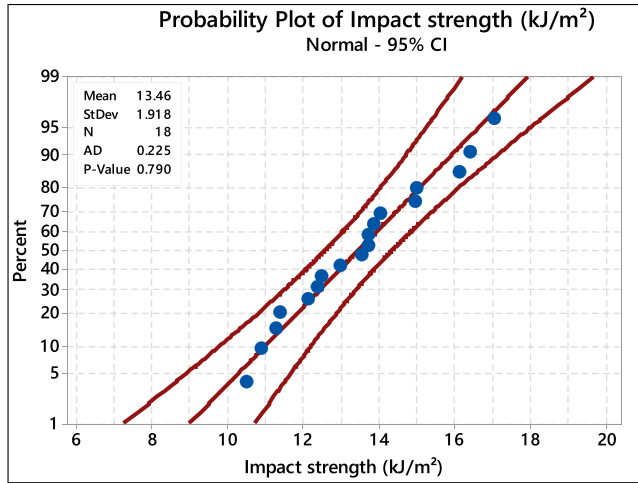


Fig. 11 – Probability plot.

were the most critical for the three-point bending strength value.

By using PLA and Re-PLA filaments, the optimum three-point bending strength modelled for the FDM process parameters was obtained at the third level of layer thickness (B3), at the first level of the filament material (A1), and at the third level of occupancy rate (C3). The main effect plot of the S/N ratios for the FDM parameters, which are effective in the three-point bending strength value, is presented in the graph in Fig. 12.

Among the process parameters used, the best values are respectively; 0.25 mm for layer thickness, 70% for occupancy rates and PLA for the filament material used. The relationship between layer thickness and occupancy rate parameters and three-point bending strength is directly proportional.

Surface plot graphs of three-point bending strength values are shown in Fig. 13. The surface plot shows the effects of layer thickness and occupancy rates, which are effective parameters on the three-point bending strength values, proportionally. Surface images are compared to understand the contribution of the parameters.

The interaction values obtained by modeling as a result of the test are presented in Table 11. The normal probability plot according to the three-point bending strength values is presented in Fig. 14. This graph is used to check the accuracy of the model. Since the p values of the normality graph are above 0.05 and the residuals follow a normal

distribution, it is understood that the experimental study and the mathematical model are compatible. In addition, the distance of the distribution from the central axis is an indicator of the stability and accuracy of the established model. The model is correct because it is a balanced distribution.

3.4. SEM analysis

Figure 15 gives the SEM images of fractured part surfaces after tests. The images were taken from the fracture areas of the material in the test result which at the fracture angle and plastic deformation regions. Quanta FEI model FEG 250 SEM device was used. Voltage of the machine is from 200V to 30 kV.

It shows the photomicrographs of the fracture surfaces of the fractured test parts during the tests. Air gaps are seen between the layers, which are responsible for the poor bonding between the layers. These cavities cause residual stresses by affecting the heat distribution during production [53]. Lower due to these gaps; it is understood that it causes the formation of tensile, three-point bending and Izod impact strength values. However, the porous structure and large voids formed on the surface reduced the resistance of the test pieces against deformation. The cross section of the fracture test parts clearly shows the parallel layers formed by the FDM process. Gaps between compounds are given in Fig. 15 in b) Surface porosity and large gaps facilitate the deformation of the test parts. As a result, the pores occurred by the filament

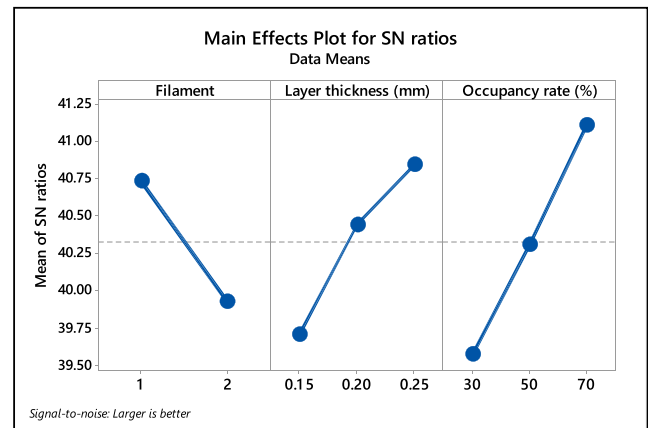


Fig. 12 – S/N rates for three-point bending strength.

Table 10 – ANOVA for S/N ratios (Three-point bending).

Factor	Degree of Freedom (DF)	Sum of Squares (SS)	Mean Square (MS)	F value	P value	Contribution (%)
A	1	466.7	466.651	47.97	0.00002	21.61
B	2	571.3	285.666	29.37	0.00002	26.46
C	2	1004.9	502.460	51.66	0.00000	46.53
Residual Error	12	116.7	9.727			5.40
Total	17	2159.6				100.00

Table 11 – Response table for S/N ratios (Larger is better).

Level	Filament	Layer thickness (mm)	Occupancy rate (%)
1	40.74	39.71	39.57
2	39.90	40.42	40.29
3	–	40.84	41.11
Delta	0.84	1.14	1.54
Rank	3	2	1

Table 12 – Prediction of Taguchi results.

Predicted Tensile Strength (MPa)	Predicted Impact Strength (kJ/m ²)	Predicted Three-point Bending Strength (MPa)
39.44	11.13	93.23
41.71	12.16	101.53
45.30	13.69	111.51
46.58	12.69	101.62
48.85	13.72	109.92
52.44	15.25	119.90
54.51	14.54	106.91
56.78	15.56	115.21
60.37	17.09	125.19
36.61	10.10	83.05
38.88	11.12	91.35
42.47	12.65	101.32
43.75	11.66	91.44
46.02	12.68	99.74
49.61	14.21	109.72
51.69	13.50	96.73
53.96	14.53	105.03
57.55	16.06	115.01

melting process throughout the PLA 3DP process reduced the strengths in the tests slightly. Because PLA filament loses some strength during production, the results were higher but like Re-PLA.

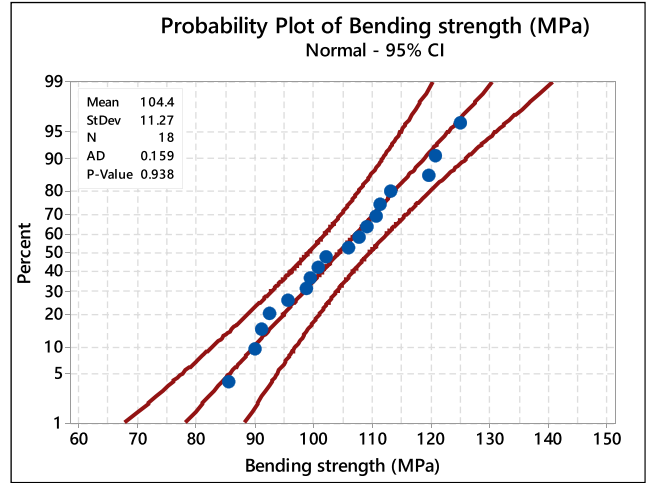


Fig. 14 – Probability plot.

In the SEM images, it appears that the PLA material is fractured in brittle behavior offering some roughness on its surface. This indicates several localized pressures that occur during fracture [54].

The finding obtained as a result of the study is that the layer thickness is the most significant factor affecting the mechanical properties. The mechanical characteristics of PLA material often rise as the layer thickness. Also, PLA is the most common used filament because it is a substance that melts at low temperatures and is an easily workable material.

In PLA materials, both virgin and recycled materials have extremely similar spectral characteristics [55].

According to the mean values, the results of the calculating Taguchi analysis were very close to the real test values (Table 12). Estimation by the mean outperformed the estimation obtained by Taguchi's logarithmic transformations. Both estimates are greater than the highest output in the experimental setup.

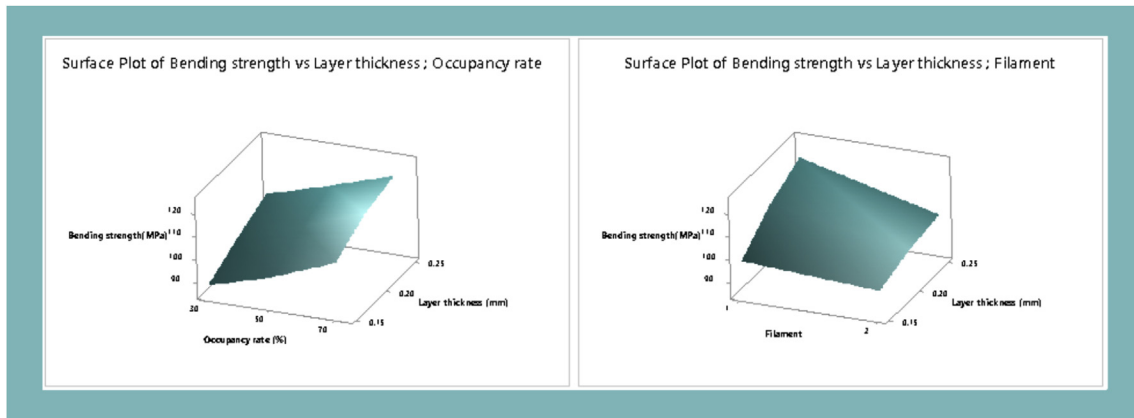


Fig. 13 – Surface plots of three-point bending strength.

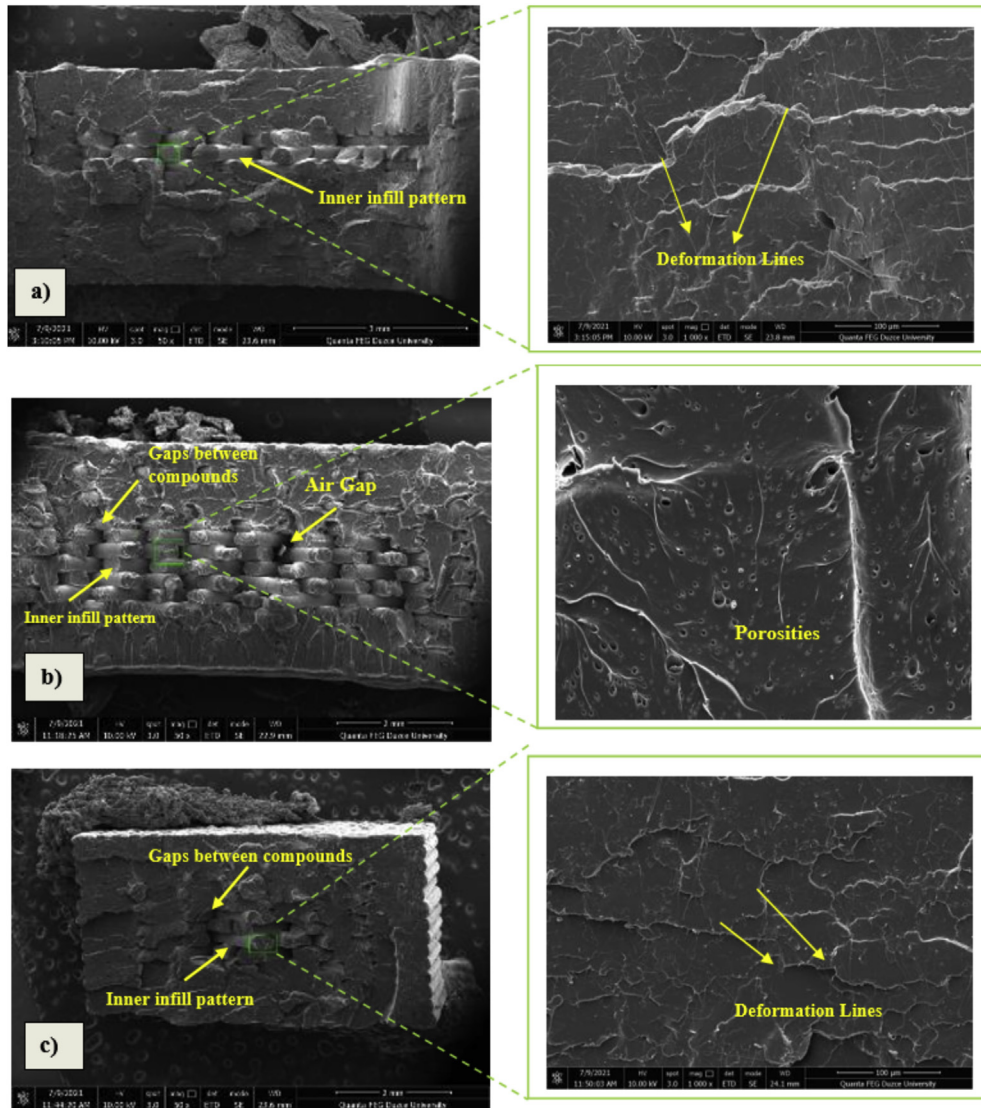


Fig. 15 – SEM images of the fractured surfaces of the optimum test pieces: a) tensile strength test part b) impact strength test part c) three point bending test part.

4. Conclusion

In this study, PLA and Re-PLA filaments and FDM from additive manufacturing techniques were used. Test parts of different production parameters; produced using layer thickness and occupancy rate. The produced test parts were subjected to tensile, izod impact and three-point bending tests. The mechanical properties obtained as a result of the test were examined experimentally and statistically. The spectrometer analysis of the Re-PLA filament revealed the presence of an additive in the filament's composition. Nozzle clogging during printing supports this finding. Apart from that, since the properties of the filament cannot be measured in detail, it is not possible to determine the individual contribution of varied factors due to the material properties.

As a result of the tests and statistical analysis; the process parameters (layer thickness, occupancy rate, and filament type) were found at 0.25 mm, 70%, and PLA, respectively. Most efficient parameter for increasing mechanical properties was

discovered to be layer thickness. It is seen that there is a decreasing trend in strength as the occupancy rate decreases.

PLA had stronger tensile strength than Re-PLA at all layer thicknesses and occupancy rates. Surface porosity and large gaps facilitate the deformation of the test parts. According to the SEM analysis, the test parts have several gaps at the location where the filament splits during the tensile test. The pores formed are due to the filament melting process during 3DP of PLA test parts. As a result of the pores created by the filament melting process during 3DP of PLA components, the strengths in the tests were lowered. The test results were higher but like Re-PLA since PLA filament lose some strength during test part production. It is possible to state that the regression model created due to the larger confidence value is useful and dependable in predicting mechanical characteristics.

All performed tests values were found to be directly proportional to occupancy rate in the study. The optimum results were 0.25 mm, 70%, and PLA for all test results; layer thickness, occupancy rates, and filament materials, respectively.

They were calculated to be 60.006 MPa, 16.961 kJ/m² at Izod impact strength, 125.423 MPa at three-point bending strength. Also, SEM has been utilized to examine the morphology and topography alterations in the fractured surface of test parts.

Air gaps were detected in SEM images. These gaps caused residual stresses by affecting the heat dissipation during production. As a result, it negatively affected the mechanical properties of the test parts.

Availability of data and materials

Not applicable.

Funding

No funding was received for conducting this study.

Authors' contributions

Gurcan ATAKOK and Menderes KAM analyzed the data of experiments and prepared the design of the study, analysis, interpretation of data and in writing the manuscript. Hanife Bukre KOC was a major contributor in writing the manuscript. All authors read and approved the final manuscript.

Declaration of Competing Interest

The authors declare that they have no known competing financial interests or personal relationships that could have appeared to influence the work reported in this paper.

REFERENCES

- [1] Yao T, Deng Z, Zhang K, Li S. A method to predict the ultimate tensile strength of 3D printing polylactic acid (PLA) materials with different printing orientations. *Compos B Eng* 2019;163:393–402.
- [2] Primo T, Calabrese M, Del Prete A, Anglani A. Additive manufacturing integration with topology optimization methodology for innovative product design. *Int J Adv Manuf Technol* 2017;93.
- [3] Pakkanen J, Manfredi D, Minetola P, Iuliano L. About the use of recycled or biodegradable filaments for sustainability of 3D printing, International Conference on Sustainable Design and Manufacturing. Springer; 2017. p. 776–85.
- [4] Turner BN, Gold SA. A review of melt extrusion additive manufacturing processes: II. Materials, dimensional accuracy, and surface roughness. *Rapid Prototyp J* 2015;21:250–61.
- [5] Parandoush P, Lin D. A review on additive manufacturing of polymer-fiber composites. *Compos Struct* 2017;182:36–53.
- [6] Saruhan H, Kam M, İpekçi A. Investigation the effects of 3D printer system vibrations on mechanical properties of the printed products. *Sigma J Eng and Nat Sci* 2018;36(3):655–66.
- [7] Aumnate APC, Pattananuwat P, Potiyaraj P. Fabrication of ABS/graphene oxide composite filament for fused filament fabrication (FFF) 3D printing. *Adv Mater Sci Eng* 2018;2018:1–9.
- [8] Gohar S, Hussain G, Ali A, Ahmad H. Mechanical performance of honeycomb sandwich structures built by FDM printing technique. *J Thermoplast Compos Mater* 2021;11:1–19. 0892705721997892.
- [9] Özdilli Ö. Comparison of the surface quality of the products manufactured by the plastic injection molding and SLA and FDM method. *Int J Eng Res Dev* 2021;13(2):428–37.
- [10] Kun K. Reconstruction and development of a 3D printer using FDM technology. *Procedia Eng* 2016;149:203–11.
- [11] Zou R, Xia Y, Liu S, Hu P, Hou W, Hu Q, et al. Isotropic and anisotropic elasticity and yielding of 3D printed material. *Compos B Eng* 2016;99:506–13.
- [12] Sachs E, Cima M, Williams P, Brancazio D, Cornie J. Three dimensional printing: rapid tooling and prototypes directly from a CAD model. 1992.
- [13] Sezer HK, Eren O, Börklü H. Carbon fiber reinforced ABS filament manufacturing and investigation of mechanical properties. 2016.
- [14] Razavykia A, Brusa E, Delprete C, Yavari R. An overview of additive manufacturing technologies—a review to technical synthesis in numerical study of selective laser melting. *Materials* 2020;13(17):3895.
- [15] Woern AL, Byard DJ, Oakley RB, Fiedler MJ, Snabes SL, Pearce JM. Fused particle fabrication 3-D printing: recycled materials' optimization and mechanical properties. *Materials* 2018;11(8):1413.
- [16] Peeters B, Kiratli N, Semeijn J. A barrier analysis for distributed recycling of 3D printing waste: taking the maker movement perspective. *J Clean Prod* 2019;241:118313.
- [17] Wach RA, Wolszczak P, Adamus-Włodarczyk A. Enhancement of mechanical properties of FDM-PLA parts via thermal annealing. *Macromol Mater Eng* 2018;303(9):1800169.
- [18] Fafenrot S, Grimmelsmann N, Wortmann M, Ehrmann A. Three-dimensional (3D) printing of polymer-metal hybrid materials by fused deposition modeling. *Materials* 2017;10(10):1199.
- [19] Ö S, Kaygusuz B. Üç boyutlu yazıcı ile üretilen PLA bazlı yapıların mekanik özelliklerinin incelenmesi. *Makina Tasarım ve İmalat Dergisi* 2006;16(1):1–6.
- [20] Wickramasinghe S, Do T, Tran P. FDM-based 3D printing of polymer and associated composite: a review on mechanical properties, defects and treatments. *Polymers* 2020;12(7):1529.
- [21] Van den Eynde M, Van Puyvelde P. 3D Printing of Poly (lactic acid). *Industrial Applications of Poly (lactic acid)* 2017:139–58.
- [22] Riaz Sundus F, Rasheed Ahmed RM, Anwar Faiza KY. Metabolic engineered biocatalyst: a solution for PLA based problems. *International journal of biomaterials* 2018:2018.
- [23] Schiavone N, Verney V, Askanian H. Effect of 3D printing temperature profile on polymer materials behavior. *3D Print Addit Manuf* 2020;7(6):311–25.
- [24] Koziar T, Mamun A, Trabelsi M, Sabantina L, Ehrmann A. Quality of the surface texture and mechanical properties of FDM printed samples after thermal and chemical treatment. *Strojnicki Vestnik/Journal of Mechanical Engineering* 2020;66(2).
- [25] Kam M, Atakok G, Koc HB. A review of mechanical and thermal properties of products printed with recycled filaments for use in 3D printers. *Surf Rev Lett* 2021. <https://doi.org/10.1142/S0218625X22300027>.
- [26] Matsuzaki R, Ueda M, Namiki M, Jeong T-K, Asahara H, Horiguchi K, et al. Three-dimensional printing of continuous-fiber composites by in-nozzle impregnation. *Sci Rep* 2016;6(1):1–7.

- [27] Ü Ç, Kam M. A review study on mechanical properties of obtained products by FDM method and metal/polymer composite filament production. *J Nanomater* 2020;2020:1–9.
- [28] A I, Kam M, Sengul O. Taguchi optimization of fused deposition modeling process parameters on mechanical characteristics of PLA+ filament material. *Sci Iran* 2021;29:79–89.
- [29] Suteja Tj SA. Mechanical properties of 3D printed Polylactic acid product for various infill design parameters: a review. In: *Journal of physics: conference series*. IOP Publishing; 2020. p. 42010.
- [30] Sheoran AJ, Kumar H. Fused Deposition modeling process parameters optimization and effect on mechanical properties and part quality: review and reflection on present research. *Mater Today Proc* 2020;21:1659–72.
- [31] Wibawa T, Mastriswadi H, Ismianti I. 3D print parameter optimization: a literature review. In: *Proceeding of LPPM UPN “veteran” yogyakarta conference series 2020—engineering and science series*; 2020. p. 146–51.
- [32] İpekçi A, Kam M., Şengül Ö., Effect of FDM process parameters on the mechanical properties and production costs of 3D printed PowerABS samples, *International Journal of Analytical, Experimental and Finite Element Analysis*, RAME Publishers 7(3) (2020) 77-90.
- [33] Vishwas M, Basavaraj C, Vinyas M. Experimental investigation using taguchi method to optimize process parameters of fused deposition Modeling for ABS and nylon materials. *Mater Today Proc* 2018;5(2):7106–14.
- [34] Mahesh V, Joladarashi S, Kulkarni SM. Development and mechanical characterization of novel polymer-based flexible composite and optimization of stacking sequences using VIKOR and PSI techniques. *J Thermoplast Compos Mater* 2019;34(8):1080–102. 0892705719864619.
- [35] Di Angelo L, Di Stefano P, Guardiani E. Search for the optimal build direction in additive manufacturing technologies: a review. *Journal of Manufacturing and Materials Processing* 2020;4(3):71.
- [36] Chamil Abeykoon, Sri-Amphorn Pimpisut, Anura F. Optimization of fused deposition modeling parameters for improved PLA and ABS 3D printed structures. *International Journal of Lightweight Materials and Manufacture* 2020;3(3):284–97.
- [37] Mahesh V, Joladarashi S, Kulkarni SM. Tribo-mechanical characterization and optimization of green flexible composites. *Emerg Mater Res* 2020;9(3):887–96.
- [38] ISO, 527. 2012 Plastics- determination of tensile strength standardization. *Book of ISO Standarts*; 2012.
- [39] Iso B. Plastics—determination of izod impact strength standardization. *ISO180*; 2000.
- [40] Watson G, Starost K, Bari P, Faisal N, Mishra S, Njuguna J. Tensile and flexural properties of hybrid graphene oxide/ epoxy carbon fibre reinforced composites. In: *IOP conference series: materials science and engineering*. IOP Publishing; 2017. p. 12009.
- [41] Horvath J, Cameron R. *Living with your 3D printer. In: Mastering 3D printing in the classroom, library, and lab*. Springer; 2018. p. 117–52.
- [42] Porima3D, *Properties of PLA Filament* <https://www.porima3d.com/porima-pla-filament>. (Accessed 17 September 2021).
- [43] Petersen EE, Kidd RW, Pearce JM. Impact of DIY home manufacturing with 3D printing on the toy and game market. *Technologies* 2017;5(3):45.
- [44] Mercan Ş. Deneysel tasarımı ve yapay zeka tekniklerinden yararlanarak ürün kalitesinin geliştirilmesi. *Balikesir Üniversitesi Fen Bilimleri Enstitüsü*; 2019.
- [45] Hintze JL. In: *PASS(Power analysis and sample size system) user’s guide I Taguchi designs*. 887. NCSS; 2008. p. 1–3.
- [46] A İ, Kam M, Şengül Ö. Investigation of the effect of FDM process parameters on mechanical properties of 3D printed PA12 samples using Taguchi method. *J Thermoplast Compos Mater* 2021;2021:1–5. 08927057211006459.
- [47] Xinhua L, Shengpeng L, Zhou L, Xianhua Z, Xiaohu C, Zhongbin W. An investigation on distortion of PLA thin-plate part in the FDM process. *Int J Adv Manuf Technol* 2015;79(5):1117–26.
- [48] Taguchi G, Phadke MS. *Quality engineering through design optimization*. In: *Quality control, robust design, and the Taguchi method*. Springer; 1989. p. 77–96.
- [49] Peace GS. *Taguchi methods: a hands-on approach*. Addison Wesley Publishing Company; 1993.
- [50] Sood AK, Ohdar RK, Mahapatra SS. Experimental investigation and empirical modelling of FDM process for compressive strength improvement. *J Adv Res* 2012;3(1):81–90.
- [51] Heidari-Rarani M, Ezati N, Sadeghi P, Badrossamay M. Optimization of FDM process parameters for tensile properties of polylactic acid specimens using Taguchi design of experiment method. *J Thermoplast Compos Mater* 2020;2020:1–8. 0892705720964560.
- [52] Saruhan H, Kam M, İpekçi A. Farklı doldurma şekillerinin üç boyutlu yazıcılarda üretilen ürünlerin mukavemetine etkisi. *Düzce Üniversitesi Bilim ve Teknoloji Dergisi* 2019;7(3):951–60.
- [53] Sood AK, Ohdar R, Mahapatra SS. Improving dimensional accuracy of fused deposition modelling processed part using grey Taguchi method. *Mater Des* 2009;30(10):4243–52.
- [54] Patanathabutr P, Soysang P, Leuang-On P, Kasetsupsin P, Hongsriphan N. A case study of recycled poly (lactic acid) contaminated with petroleum-based thermoplastics used in packaging application. *Key Eng Mater* 2019:279–84. *Trans Tech Publ*.
- [55] Pinho AC, Amaro AM, Piedade AP. 3D printing goes greener: study of the properties of post-consumer recycled polymers for the manufacturing of engineering components. *Waste Manag* 2020;118:426–34.